Direct evidence of defect annihilation during structural relaxation of amorphous indium phosphide

G. de M. Azevedo*
Department of Electronic Materials Engineering, Research School of Physical Sciences and Engineering, The Australian National University, GPO box 4, Canberra, ACT 0200, Australia

C. J. Glover
Max-Lab, Lund University, Box 118, Lund, Sweden

M. C. Ridgway
Department of Electronic Materials Engineering, Research School of Physical Sciences and Engineering, The Australian National University, GPO box 4, Canberra, ACT 0200, Australia

K. M. Yu
Materials Science Division, Lawrence Berkeley National Laboratory, Berkeley, California 94720, USA

G. J. Foran
Australian Nuclear Science and Technology Organisation, Menai, Australia
(Received 14 April 2003; revised manuscript received 30 June 2003; published 25 September 2003)

Extended x-ray absorption fine structure measurements have been used to characterize the low-temperature, thermally induced structural relaxation of amorphous InP. We show reductions in both chemical and structural disorder associated with homopolar and heteropolar bonding, respectively, are operative during structural relaxation of this amorphous compound semiconductor. The latter is analogous to that observed in the amorphous elemental semiconductors Ge and Si. Though a reduction in homopolar bonding accompanies structural relaxation, the fully relaxed, minimum-energy configuration of the amorphous phase still retains chemical disorder.

DOI: 10.1103/PhysRevB.68.115204 PACS number(s): 61.10.Ht, 61.43.Dq, 61.72.Vv, 61.72.Cc

I. INTRODUCTION

Despite several decades of study, a definitive picture of the structure of amorphous semiconductors has yet to be achieved. For example, in compound semiconductors, basic concepts such as the extent of homopolar bonding are still under debate.[1–7] From the theoretical point of view, their presence is strongly dependent on the computational approach utilized while, from the experimental point of view, sample artifacts such as voids, inhomogeneities and deviations from stoichiometry impede an accurate structural characterization. Even in the absence of such artifacts, the nonequilibrium processes utilized for the preparation of amorphous semiconductors (i.e., deposition, sputtering, evaporation, or ion implantation) can yield a preparation-specific structure with a free energy greater than that of the intrinsic, minimum-energy configuration of the amorphous phase. Such excess energy is accommodated in the form of defects such as undercoordinated and overcoordinated atoms or homopolar bonds, and deviations from the ideal bonding configurations, in the form of bond bending and bond stretching distortions. Upon low temperature annealing, the concentration of defects and energetically unfavorable configurations can be lessened as the amorphous phase relaxes to a lower-energy variant. The amorphous phase can thus accommodate a range of configurations with energy above that of the ''minimum-energy'' amorphous state.

During thermal annealing of amorphous Si and Ge, the structural ordering observed prior to crystallization (termed structural relaxation) has been studied with a variety of techniques including Raman scattering,[8] differential scanning calorimetry (DSC),[9,10] and extended x-ray absorption fine structure (EXAFS) spectroscopy.[11,12] For amorphous Ge, the heat release of 6 KJ/mol (one half the crystallization enthalpy) measured with DSC (Ref. 13) was concomitant with the reduction in the width of the bond-angle and bond-length distributions, as measured with Raman[8] and EXAFS,[11] respectively. Two possible scenarios for structural relaxation were proposed.[8,9] In the first, it was assumed that the excess enthalpy arose from strain energy stored in the form of bond-angle distortions in a fully coordinated continuous random network (CRN) and structural relaxation involved reordering of the CRN as a whole.[8] In the second, the heat release was considered a local phenomenon that arose from point-defect annealing in a defective CRN that was also accompanied by a reduction in bond-angle distortion.[9] The isothermal calorimetry experiments of Roorda *et al.*[9] provided compelling evidence in support of the second scenario, showing the transient heat release during structural relaxation of amorphous Si obeyed bimolecular reaction kinetics characteristic of a point-defect annihilation mechanism. Recently, Glover *et al.*[12] utilized Raman and EXAFS measurements to show that structural relaxation in amorphous Ge involved both bond-angle and bond-length ordering again consistent with point-defect annealing. Structural relaxation has also been observed in ion-damaged and amorphous compound semiconductors.[14–16] Cliche *et al.* reported structural relaxation of amorphous InP at room temperature including a vol-

ume expansion partly accommodated by shear plastic flow.[15] Analysis of the annealing kinetics[15] and measurements of the viscosity as a function of relaxation time[16] were considered indicative of structural relaxation controlled by point-defect annealing. Despite these detailed studies, the specific atomistic mechanisms governing structural relaxation of the amorphous phase of both elemental and compound semiconductors have yet to be identified.

Our aims in this paper are twofold. First, we investigate the means of structural relaxation in an amorphous compound semiconductor and determine whether this process is a local phenomenon, proceeding via point-defect annihilation,[9] or alternatively whether structural relaxation involves the topological reorganization of the system as a whole.[8] Second, following structural relaxation, we characterize the minimum free-energy structure of the amorphous phase at the atomic scale. We focus particular attention on the identification and quantification of chemical disorder, manifested in the form of homopolar bonds. In a previous report, Glover *et al*. identified homopolar bonds in compound semiconductors amorphized by ion implantation.[4] However, whether homopolar bonds are intrinsic to the structure of amorphous compound semiconductors or are a preparation-specific artifact resulting from the nonequilibrium nature of the ion implantation process has yet to be determined. Given homopolar bonds yield a significant number of midgap states[17] and hence influence the optical, electronic, and vibrational properties of amorphous compound semiconductors, such measurements are crucial to fully exploit these technologically important materials. To accomplish our goals, we utilized an appropriate materials system in combination with advanced processing and characterization techniques. We present results for amorphous InP given the previous reports of structural relaxation studied with alternative methodologies[14–16] and the high atomic-number contrast that enabled quantification of homopolar bonding.[4] Furthermore, we used a preparation technique that yielded stoichiometric, homogeneous and void-free samples for EXAFS analysis.[4,5] The latter is ideally suited for the determination of the atom-specific, short-range-order parameters in amorphous materials including coordination number, bond length and static and thermal disorder.

II. EXPERIMENT

The sample preparation method utilized in this report is a modification of that first described in Refs. 4 and 5. Polycrystalline InP layers of thickness 3 μm were deposited on (100) Si substrates of thickness 350 μm by metalorganic chemical vapor deposition. Multiple-energy, multiple-dose P implantations, with the ion doses scaled to yield a constant energy deposited in vacancy production to a depth 3.5 μm, were used to amorphize the polycrystalline InP layer. Ion doses and energies are summarized in Table I. During implantation, samples were maintained at liquid-nitrogen temperature to inhibit dynamic annealing. Though the total implanted dose was approximately two orders of magnitude greater than that necessary to amorphize the polycrystalline layer, the resulting deviation from stoichiometry (0.5 at. %) was negligible relative to the sensitivity of the analysis method. To produce samples appropriate for transmission-mode EXAFS measurements, the Si substrate thickness was subsequently reduced to 15 μm by mechanical grinding. To inhibit diffraction effects, samples were then finely crushed and mixed with a BN binder. The total amount of material was such that $\mu x = 1$ where μ is the energy-dependent attenuation factor and x is the effective sample thickness. Transmission EXAFS measurements were performed at a temperature of 10 K, at beamline 7-3 of the Stanford Synchrotron Radiation Laboratory. Such measurements were performed one week after sample preparation. Absorption spectra were recorded at the In *K*-edge (27.940 keV), using a Si (220) double crystal monochromator with nominal energy resolution $\Delta E/E \sim 10^{-4}$. Harmonic rejection was accomplished by detuning the monochromator by 30%. The origin of the energy scale (E_0) was set as the maximum of the derivative of the absorption edge. EXAFS spectra were isolated from the raw absorption data by pre-edge and post-edge background subtraction with the ''Spline'' module of the XFIT code.[18] Displayed in Fig. 1(a) are typical spectra of k^3-weighted fine structure as a function of photoelectron momentum k while Fig. 1(b) shows spectra Fourier-transformed over a k range of 2–16 Å $^{-1}$.

TABLE I. Summary of the implantation conditions (doses and energies) utilized to amorphize the InP samples.

Energy (keV)	Dose (ions/cm^2)
100	2.5×10^{15}
400	3.1×10^{15}
700	3.1×10^{15}
1000	3.7×10^{15}
2000	3.7×10^{15}
3000	6.1×10^{15}
5000	6.1×10^{15}
7000	8.0×10^{15}
8500	8.0×10^{15}

The EXAFS spectrum of the polycrystalline sample displays a complicated structure consistent with the superposition of different frequency components as confirmed by the corresponding Fourier-transformed spectrum which shows the presence of multiple peaks attributable to first, second and third nearest neighbors. In contrast, the spectrum for the as-implanted sample is dominated by a single frequency component, the result of photoelectron scattering from a single shell. Clearly, the structural disorder introduced by the ion implantation process is sufficient to damp out coherent scattering from beyond the first shell.

The as-implanted sample was subsequently annealed isochronally (1 h) over a temperature range of 100–270 °C ($\pm$10 °C). After each annealing step, absorption spectra were recorded as above (variation from sample to sample was thus eliminated by sequentially annealing the same sample). Included in Fig. 1(b) are Fourier-transformed spectra following annealing at 200 and 237 °C. Relative to the as-implanted sample, the amplitude of the first nearest-neighbor peak in-

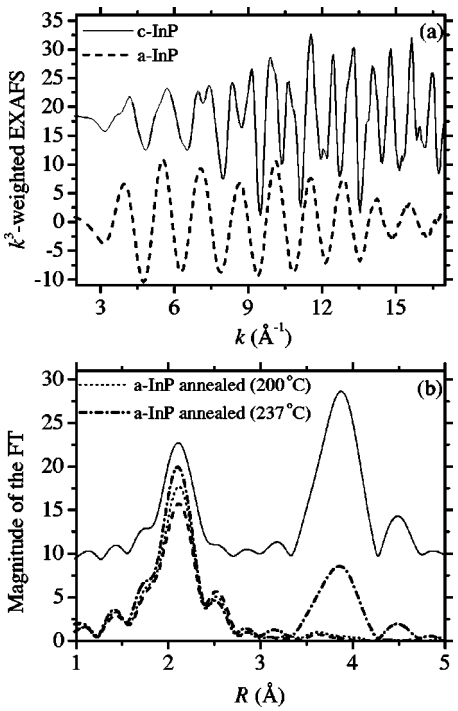

FIG. 1. (a) k^3-weighted EXAFS spectra for polycrystalline (c-InP) and amorphized InP (a-InP) (solid and dashed lines, respectively) as a function of photoelectron momentum k. (b) Fourier transforms of the spectra shown in panel (a), as a function of non-phase-corrected radial distance. Also shown, are Fourier transforms for amorphous samples annealed at 200 and 237 °C (dotted and dashed-dotted lines, respectively). For clarity of presentation, the spectra for polycrystalline InP have been offset vertically and the EXAFS and Fourier transforms for the amorphous samples have been multiplied by 3 and 2, respectively.

creases with annealing temperature. We note the presence of a second nearest-neighbor contribution after annealing at 237 °C, indicative of the onset of crystallization, and estimate the crystalline volume fraction for this sample was 20%. The sample is clearly amorphous for annealing temperatures up to 200 °C.

III. DATA ANALYSIS

We have utilized multiparametric, nonlinear least-squares fitting via the IFEFFIT code[19] with single-scattering and Gaussian approximations. The phase and backscattering amplitude were calculated *ab initio* with the FEFF8.0 code.[20] Fittings were performed in k space in the range of $2-16$ Å^{-1} with the filtered EXAFS obtained via back-Fourier transformation over a non-phase-corrected radial range of 1.5–2.9 Å. To minimize the number of free parameters during structural refinement, the amplitude reduction factor (S_0^2) and the threshold energy (E_0) were determined from the polycrystalline InP reference sample and held constant during analysis of the amorphous samples. The parameters obtained in the fitting of the crystalline standard are listed in Table II.

The nature of disorder in amorphous compound semiconductors is more complex than in their elemental counterparts, given the potential presence of chemical disorder manifested

TABLE II. Refined parameters obtained for the polycrystalline standard (c-InP), as-implanted (25 °C) and annealed (200 and 237 °C) amorphous InP. CN, BL, and DWF stand for coordination number, bond length, and Debye-Waller factor, respectively.

	c-InP	As-implanted (25 °C)	Annealed (200 °C)	Annealed (270 °C)
In-P CN	4	3.2 $\pm$0.2	3.4 $\pm$0.1	3.9 $\pm$0.2
In-P BL (Å)	2.526 $\pm$0.002	2.551 $\pm$0.002	2.544 $\pm$0.002	2.527 $\pm$0.002
In-P DWF(Å^2)	0.0022 $\pm$0.0002	0.0044 $\pm$0.0003	0.0040 $\pm$0.0002	0.0022 $\pm$0.0002
In-In CN		0.7 $\pm$0.1	0.6 $\pm$0.1	
In-In BL (Å)		2.757 $\pm$0.004	2.745 $\pm$0.004	
In-In DWF(Å^2)		0.006 $\pm$0.002	0.006 (constrained)	

in the form of homopolar bonds. A detailed examination of Fig. 1(a) reveals beats in the EXAFS amplitude for amorphized InP, characteristic of a first nearest-neighbor shell comprised of two different bond lengths.[4] Accordingly, the model utilized during structural refinement of the amorphous samples consisted of a mixed first shell, comprised of P and In scatterers, necessitating six fitting parameters (bond lengths, coordination numbers, and, Debye-Waller factors).

Though the number of fitting parameters is smaller than the number of independent points in the experimental data (11, as estimated from Nyquist formula[21]), the correlation between the In-In coordination number and Debye-Waller factor was 0.95 or greater. Thus, these two parameters could not be determined independently, i.e., only five parameters can be simultaneously refined. For that reason, we fixed the In-In Debye-Waller factor at 0.006 Å^2, the value determined for the as-implanted sample when refining the six parameters simultaneously. While this procedure potentially yields an underestimation of the absolute number of In-In bonds, it provides a more robust evaluation of the relative changes in their number, as a function of annealing temperature.

Figures 2(a) and 2(b) show fitted and experimental filtered (back-transformed) EXAFS and Fourier-transformed spectra, respectively, for the as-implanted and annealed samples, together with contributions due to In-P and In-In bonds. Clearly, the fitting to the experimental data is good in both k and R space, over the given windowed ranges of $2-16$ Å^{-1} and 1.5–2.9 Å , thus confirming the multielemental nature of the first shell.

IV. RESULTS AND DISCUSSION

Coordination numbers, bond lengths and Debye-Waller factors are plotted as functions of temperature in Fig. 3(a), 3(b), and 3(c), respectively. Error bars were determined by standard methods.[19] For the as-implanted sample, we note the In environment remains approximately fourfold coordi-

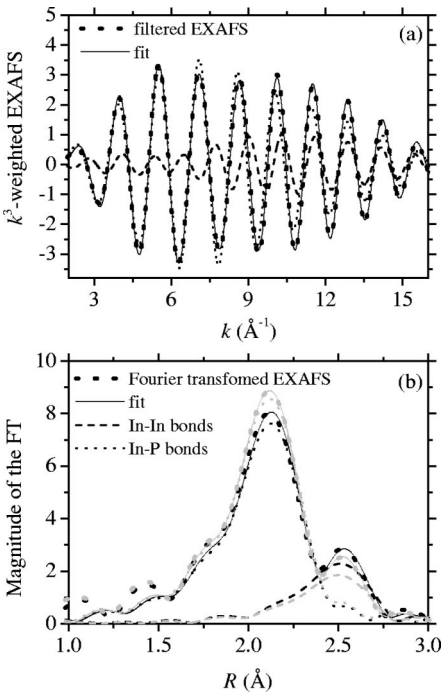

FIG. 2. (a) Filtered (back-transformed) EXAFS spectra as a function of photoelectron momentum for the as-implanted sample. (b) Magnitude of the Fourier transforms for the first coordination shell as a function of non-phase-corrected radial distance for as-implanted and annealed (200 °C) samples. Thick-dashed lines are the experimental data, solid lines are the fitting results, and thin-dashed and dotted lines are the contributions due to In-In and In-P bonds. Black and gray lines correspond to the as-implanted and annealed samples, respectively.

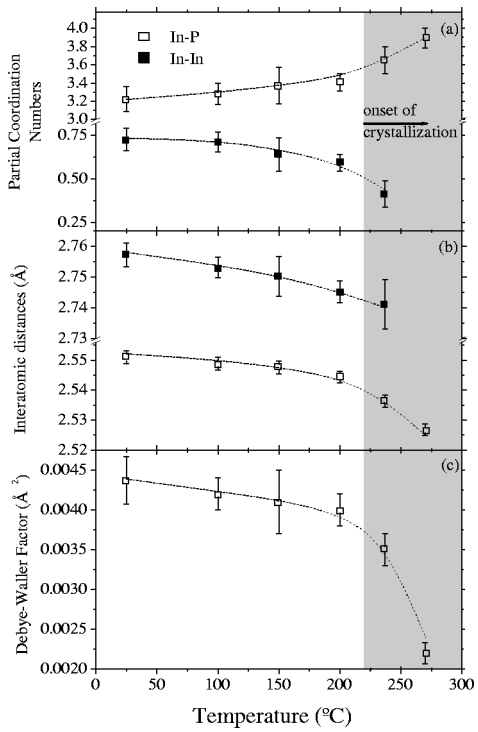

FIG. 3. Structural parameters as a function of annealing temperature including coordination numbers (a), bond lengths (b), and Debye-Waller factors (c). The dotted lines are a guide to the viewer's eye. The shaded area indicates the presence of crystallites in the annealed samples.

nated with an average of 3.9 ± 0.3 neighbors comprised of 3.2 ± 0.2 P atoms and 0.7 ± 0.1 In atoms. Given the trivalence of In, O'Reilly *et al.* suggested threefold coordinated atoms are the most common structural defect in amorphous InP,[17] potentially yielding undercoordination (<4 atoms). In contrast, Lewis *et al.* anticipated the over coordination of In atoms (3.91 P atoms and 0.34 In atoms surrounding each In atom).[22] The experimental uncertainty associated with the results presented herein impedes our ability to unambiguously identify an under or overcoordinated In environment. Relative to the polycrystalline standard, the In-P bond length and Debye-Waller factor in the amorphous phase increase by 1 and 100%, respectively, the latter consistent with an increase in static disorder [we have reported similar observations for amorphous GaAs (Ref. 5) and InAs (Ref. 23)]. An increase in the In-P bond length is expected given the shape of the interatomic potential near the equilibrium distance and reflects the means by which the amorphous network accommodates the elastic deformation due to the presence of structural and chemical disorder. Calculations by Lewis *et al.*, predict the In-P bond length in amorphous InP should increase by 2%, relative to the crystalline phase,[22] in qualitative agreement with our results. Finally, the In-In bond length is 2.76 Å, consistent with that expected from the In covalent radius (1.4 Å).[24]

The results presented above for the as-implanted sample unequivocally demonstrate the presence of In-In bonds in amorphous InP. Homopolar bonds have been reported in previous EXAFS experiments that characterized the structure of amorphous InP prepared by flash evaporation[6] and deposition.[7] However, the samples investigated were highly nonstoichiometric with an excess of P atoms. The proportion of wrong bonds was reported to be between 10% and 40%, as a result, the origin of the homopolar bonding was not clear. Flank *et al.*[6] have suggested that the system partly phase separated (due to clustering of excess P atoms) while Udron *et al.* indicated that P is more or less uniformly distributed in the samples, but suggested that wrong bonds were due to local composition fluctuations rather than the presence of topological defects.[7]

Phase separation or local compositional fluctuations are unlikely causes of the presence of homopolar bonding reported herein. First, recall that the amorphous samples were produced by ion implantation into stoichiometric polycrystalline InP. Secondly, the In-In bond lengths are consistent with covalent bonds between In atoms. If small metallic In clusters were present, we would have expected to observe longer metallic In-In bonds ($\sim$3.2 Å). Thirdly, additional experiments indicate the as-implanted structure of amorphous InP is independent of the total implanted ion dose over more than two orders of magnitude above the amorphization threshold, with no observable variation in the number of In-In bonds.[25] The latter result indicates that an 18% In-In bonding fraction is intrinsic to the as-implanted amorphous

phase of InP and does not stem from extrinsic effects such as phase separation or local compositional fluctuations.[25]

Upon annealing, a clear reduction in the In-P and In-In bond lengths, as well as changes in the Debye-Waller factor associated with In-P bonds are observed, consistent with a thermally induced reduction in static disorder. The number of homopolar (heteropolar) bonds decreases (increases), as consistent with a thermally induced reduction in chemical disorder. At 200 °C, In-In homopolar bonding is reduced by 20% relative to the as-implanted sample.

Should the In-In Debye-Waller Factor decrease in a manner similar to that observed for In-P bonding, the reduction in In-In bonding would be *greater* than that quoted in Fig. 3. Therefore, we note that having constrained the Debye-Waller factor associated with In-In bonding, 20% is thus the *minimum* relative change in the In-In coordination number resulting from structural relaxation. Finally, we also note the structural parameters after annealing at 270 °C are the same (within error bars) as those for the polycrystalline reference (see Table II), i.e., the sample has recrystallized.

Figure 3 establishes two important facts. First, structural relaxation of amorphous InP proceeds via the reduction of both chemical and static disorder associated with homopolar and heteropolar bonding, respectively. The reduction in the In-In bonding fraction identifies defect annihilation in the amorphous phase. Second, despite the observed reduction in chemical disorder, the fully relaxed (200 °C annealing) amorphous structure *retains* a significant homo-polar bonding fraction (15%) as consistent with the calculations of Lewis *et al.*[22] Equivalently, homopolar bonding is *intrinsic* to the amorphous phase.

The changes in the structural parameters due to annealing, as presented in Fig. 3, are subtle. As noted previously, we minimized experimental error by utilizing the same sample for all measurements of the amorphous-phase structure and fixed as many free parameters as possible during structural refinement. Nonetheless, the validity of our observations can be confirmed by a model-independent means. Specifically, by analysis of the phase difference $\Delta\Phi=\Phi_c-\Phi_a$ between the filtered, back-transformed EXAFS for polycrystalline (Φ_c) and annealed samples (Φ_a) as a function of photoelectron momentum *k*. Figure 4 shows such a plot for the given annealing conditions. A fully recrystallized sample with structural parameters identical to that of the first nearest neighbor of the polycrystalline standard would yield a phase difference of zero over the entire *k* range examined. Clearly, the phase difference decreases over the entire *k* range as the annealing temperature increases and the sample becomes more ''crystalline-like.'' Similar trends are apparent in plots of the logarithm of the ratio of the amplitudes of the filtered EXAFS for polycrystalline and amorphous samples, as a function of k^2 (not shown). These systematic changes in the phase difference and amplitude ratio confirm our ability to identify the subtle annealing-induced changes in the structural parameters presented above. Although changes in bond lengths, Debye-Waller factors and coordination numbers occur concomitantly during thermal annealing, Fig. 4 can be utilized as model-independent evidence of homopolar bond annihilation during structural relaxation, as follows. In Fig. 2(a), the filtered EXAFS corresponding to In-P and In-In bonds have comparable amplitudes in the *k* range above 10 Å $^{-1}$. At lesser *k* values, the filtered EXAFS is dominated by the In-P contribution. We also note that the In-P and In-In contributions are out of phase at $k=7.0$ Å $^{-1}$. Given In-In bonds are absent in the polycrystalline standard, the annihilation of In-In bonds during structural relaxation of amorphous InP should yield the greatest change in the phase difference (Fig. 4) at *k* values around 7 and above 10 Å $^{-1}$. Such changes are readily apparent and progressively increase with annealing temperature. This analysis in conjunction with the Fourier-transformed spectra and the structural parameters presented in Fig. 2(b) and 3(a)–3(c), respectively, demonstrate the removal of homopolar bonds during the thermally induced structural relaxation of amorphous InP. To our knowledge, this represents the first identification of a specific defect annihilation mechanism associated with the relaxation process. Although annihilation of point defects such as undercoordinated and overcoordinated atoms are possibly operative during structural relaxation, the identification of annihilation of the latter point defects is impeded by the error bars associated with coordination numbers, listed in Table II.

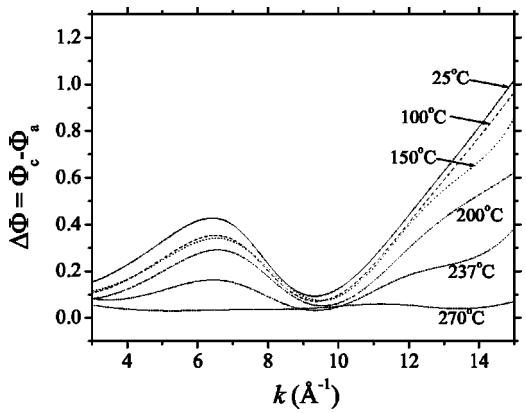

FIG. 4. Phase difference $\Delta\Phi=\Phi_c(k)-\Phi_a(k)$ between the phase of the filtered EXAFS for the polycrystalline standard $[\Phi_c(k)]$ and the annealed samples $[\Phi_a(k)]$, as a function of the photoelectron momentum *k*.

The presence of homopolar bonds suggests odd-membered rings exist in the topology of the amorphous phase. Although their presence cannot be proven directly from our data, the connection between wrong bonds and odd-membered rings in amorphous InP is supported by the calculations of Lewis *et al.*, which predict a significant fraction of five- and seven-membered rings.[22] The latter are the most frequent in the topology (4.37 per atom) followed by the crystalline-type six-membered rings (2.35 per atom).[22] Five-, four-, and three-membered rings are also present, but in lesser amounts (<0.5 per atom).[22] Based on the calculations by Lewis, we speculate the reduction of homopolar bonding demonstrated in the present experiment is consistent with a reduction in the numbers of five- and seven-membered rings.

Raman scattering and EXAFS[8,11,12] have been previously utilized to characterize structural relaxation in amorphous Si

and Ge. A concomitant reduction in bond length and width of the bond-length and bond-angle distributions was reported. The relaxation of amorphous elemental Si and Ge thus presents several similarities to the relaxation of the amorphous compound semiconductor InP. Concomitant to a reduction in homopolar bonding, we observe a reduction in bond length and Debye-Waller factor associated with heteropolar bonding. For compound semiconductors, heteropolar bonding is characteristic of the crystalline phase. During structural relaxation of the amorphous phase, the reduction in disorder associated with the ''crystalline-type'' bonding is thus common to both compound and elemental semiconductors. This reduction in structural disorder yields a decrease in residual strain or elastic energy while reduction in chemical disorder yields a decrease in both elastic and Coulombic energy, the latter due to partial ionic character of the bonding in InP.

Cliche *et al.* have shown as-implanted amorphous InP is 0.5% denser than the crystalline phase.[14–16] Lewis *et al.*[22] suggested the overcoordination of both In and P environments could be a potential cause for a denser amorphous phase. As we have discussed above, the data presented herein cannot unambiguously identify whether the In environment is undercoordinated or overcoordinated. At first glance, the presence of In-In bonds (which are longer than In-P bonds) suggests a less dense amorphous phase. Nevertheless, a simple calculation shows that our data can be consistent with that of Cliche *et al.* Our results clearly indicate covalent In-In bonds are present in the amorphous InP. It is thus reasonable to assume P-P bonds [with bond length of 2.2 Å (Ref. 24)] also exist in the amorphous network. With this assumption and the structural parameters listed in Table II for the as-implanted InP sample, it is trivial to show that a 0.5% denser amorphous phase requires the presence of 0.85 P-P bonds per P atom (with the 3.2 In-P bonds per P atom as above). This is a reasonable number given the present data indicates a comparable number of In-In bonds (0.7 per In atom). The above discussion highlights the importance of a detailed structural characterization of the atomic environment surrounding P atoms in amorphous InP. Such experiments are underway.

V. CONCLUSIONS

In summary, we have demonstrated that structural relaxation of amorphous InP proceeds via the reduction of both chemical and structural disorder. We have also shown that the fully relaxed amorphous-phase structure of InP retains homopolar bonding confirming that chemical disorder is not a preparation-specific artifact, being intrinsic to the minimum-energy structure of amorphous compound semiconductors. Furthermore, our quantitative measurements of the extent of homopolar bonding were consistent with recent, first-principles calculations.

ACKNOWLEDGMENTS

G.M.A. acknowledges the Brazilian agency CNPq (Conselho Nacional de Desenvolvimento Científico e Tecnológico) for financial support. G.M.A., M.C.R., and G.J.F. were supported by the Australian Synchrotron Research Program, which is funded by the Commonwealth of Australia via the Major National Research Facilities Program. K.M.Y. was supported by the Office of Science, Office of Basic Energy Science, Division of Materials Sciences and Engineering, of the US Department of Energy under Contract No. DE-AC03-76SF00098. The Stanford Synchrotron Radiation Laboratory is supported by the Office of Basic Energy Sciences of the US Department of Energy.

*Electronic address: azevedo@lnls.br

[1] N. Mousseau and L. J. Lewis, Phys. Rev. Lett. **78**, 1484 (1997).
[2] N. Mousseau and G. T. Barkema, Phys. Rev. B **61**, 1898 (2000).
[3] H. Seong and L. J. Lewis, Phys. Rev. B **53**, 4408 (1996).
[4] C. J. Glover, M. C. Ridgway, K. M. Yu, G. J. Foran, T. W. Lee, Y. Moon, and E. Yoon, Appl. Phys. Lett. **74**, 1713 (1999).
[5] M. C. Ridgway, C. J. Glover, G. J. Foran, and K. M. Yu, J. Appl. Phys. **83**, 4610 (1998).
[6] A. M. Flank, P. Lagarde, D. Udron, S. Fisson, A. Gheorghiu, and M. -L. Thèye, J. Non-Cryst. Solids **97&98**, 435 (1987).
[7] D. Udron, A. M. Flank, P. Lagarde, A. Raoux, and M. -L. Thèye, J. Non-Cryst. Solids **150**, 361 (1992).
[8] J. Fortner and J. S. Lannin, Phys. Rev. B **37**, 10 154 (1988).
[9] S. Roorda, W. C. Sinke, J. M. Poate, D. C. Jacobson, S. Dierker, B. S. Dennis, D. J. Eaglesham, F. Spaepen, and P. Fuoss, Phys. Rev. B **44**, 3702 (1991).
[10] S. Roorda, S. Doorn, W. C. Sinke, P. M. L. O. Scholte, and E. van Loenen, Phys. Rev. Lett. **62**, 1880 (1989).
[11] C. E. Bouldin, R. A. Forman, M. I. Bell, and E. P. Donovan, Phys. Rev. B **44**, 5492 (1991).
[12] C. J. Glover, M. C. Ridgway, K. M. Yu, G. J. Foran, D. Desnica-Frankovic, C. Clerc, J. L. Hansen, and A. Nylandsted-Larsen, Phys. Rev. B **63**, 073204 (2001).
[13] E. P. Donovan, F. Speapen, D. Turnbull, J. M. Poate, and D. C. Jacobson, J. Appl. Phys. **57**, 1795 (1985).
[14] L. Cliche, S. Roorda, G. E. Kajrys, and R. A. Masut, J. Appl. Phys. **79**, 2142 (1996).
[15] L. Cliche, S. Roorda, and R. A. Masut, Appl. Phys. Lett. **65**, 1754 (1994).
[16] L. Cliche, S. Roorda, and R. A. Masut, Nucl. Instrum. Methods Phys. Res. B **96**, 319 (1995).
[17] E. P. O'Reilly and J. Robertson, Phys. Rev. B **34**, 8684 (1986).
[18] P. J. Ellis and H. Freeman, J. Synchrotron Radiat. **2**, 190 (1995).
[19] M. Newville, J. Synchrotron Radiat. **8**, 322 (2001).
[20] A. L. Ankudinov, B. Ravel, J. J. Rehr, and S. D. Conradson, Phys. Rev. B **58**, 7565 (1998).
[21] L. Brillouin, *Science and Information Theory* (Academic, New York, 1967), p. 94.
[22] L. J. Lewis, A. de Vita, and R. Car, Phys. Rev. B **57**, 1594 (1998).
[23] G. de M. Azevedo, M. C. Ridgway, K. M. Yu, C. J. Glover, and G. J. Foran, Nucl. Instrum. Methods Phys. Res. B **190**, 851 (2002).
[24] J. A. Van Vechten and J. C. Philips, Phys. Rev. B **2**, 2160 (1970).
[25] G. de M. Azevedo *et al.* (unpublished).